Heliyon 9 (2023) e13047

Contents lists available at ScienceDirect

Heliyon

journal homepage: www.cell.com/heliyon

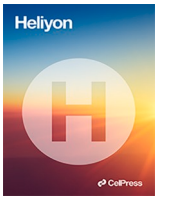

Research article

Spatio-temporal assessment of the impacts of the trends in physical and biogeochemical parameters on the primary production of the Gulf of Guinea

Adeola M. Dahunsi [a,*], Tolulope S. Oyikeke [b,c], Mujeeb A. Abdulfatai [a,d], Lateef A. Afolabi [e,f]

[a] University of Abomey-Calavi, Cotonou, Benin
[b] Department of Climate Change and Marine Sciences, Universidade Técnica do Atlântico (UTA)–ISECMAR, Cape Verde
[c] West African Science Service Centre on Climate Change and Adapted Land Use (WASCAL), Cape Verde
[d] Alfred-Wegener-Institute Helmholtz Centre for Polar- and Marine Research, Bremerhaven, Germany
[e] Department of Fisheries and Aquatic Sciences, University of Cape Coast, Cape Coast, Ghana
[f] Centre for Coastal Management-Africa Centre of Excellence in Coastal Resilience, University of Cape Coast, Cape Coast, Ghana

ARTICLE INFO

Keywords:
Coastal waters
Gulf of Guinea
Climate change
Models
Primary productivity
Phytoplankton
Nutrients
Trends

ABSTRACT

This study applied ocean models data from Copernicus Marine Environment Monitoring Service (CMEMS) in assessing the impacts of the trends in key ocean parameters on the primary production of the Gulf of Guinea (GoG). Trend analyses, from 1993 to 2020, were done using linear regression and Mann-Kendall significance test methods to ascertain inter-annual and inter-seasonal variations and check the significance of the trends, respectively. Results affirm that temperature, salinity, nutrients, and oxygen play significant roles in the primary production of the GoG. Also, parameters such as temperature, salinity, chlorophyll-A, net primary production, phosphate, and dissolved oxygen have been experiencing increases between the study duration while silicate and nitrate have been declining in the GoG. However, there are regions and years with contrary values to the average trends. The varying level of significance of the trend showed that the impacts of the climate on the primary production of the GoG vary basin-wide.

1. Introduction

It is generally known that marine food web relies to a great extent on the phytoplankton primary production as it accounts for an estimated 95% of marine primary production [1,2]. Hence, a change in this important source of food to the higher trophic levels will have effects of varying magnitudes on the wellbeing of the marine ecosystem [3]. Global marine primary production of about 50–60 pentagrams of Carbon per year [4,5] has been reported by global and regional studies. The abundance or scarcity of the primary producers regulate fish catch thereby increasing or reducing the volume of protein available to humans use [5]. This primary production provide support principally for all life in the oceans and ultimately affects global biogeochemical cycles and climate [5].

These photosynthetic phytoplankton also contribute to climate regulations by absorbing more than 100 Teragram of carbon per day [6]. This reduces the global temperature because it removes more CO_2, a renowned greenhouse gas, from the atmosphere [7]. It is

* Corresponding author.;
E-mail addresses: dahunsi_adeola@yahoo.com, dahunsi_adeola_michael@cipma.net (A.M. Dahunsi).

https://doi.org/10.1016/j.heliyon.2023.e13047
Received 12 May 2022; Received in revised form 5 January 2023; Accepted 12 January 2023
Available online 18 January 2023

reported that the ocean takes up about 30% of the annual anthropogenic emissions [8]. Climate change has been reported to be the biggest anthropogenic threat faced by marine ecosystem [9]. Study have reported a significant increase in Sea Surface Temperature (SST) in the global ocean [10]. This has led to an increased thermal gradient between the surface water and the layer below which is expected to cause a reduction of nutrients supplied to the surface layer where primary production is predominant [11]. Similarly, studies have found that increasing SST has been implicated in the observed decline of oceanic phytoplankton biomass and other biological effect on plankton metabolic rates [12,13]. This has consequently reduced the climate regulating role of the global ocean through CO_2 capture by photosynthetic phytoplankton [14]. Other impacts of climate change on the global ocean include a change in nutrient supply [15].

Unlike the less productive open ocean, the coastal seas like the Gulf of Guinea (GoG) coastal waters contributes close to 80% of the global seafood harvested from the wild [16]. The upwelling system of West Africa combined with that of the western Iberian Peninsula has been reported to be one of the largest marine ecosystems globally [17]. It supports a high quantity of fisheries and aquaculture because of the high nutrients inputs from coastal sources and upwelling [18,19]. Despite these important contributions, the coastal seas have been the most impacted by human activities including overfishing, marine transport and engineering activities, plastic and agricultural pollution in form of nutrient enrichment [20,21].

Several factors such as temperature, light and nutrient availability have been linked to marine primary production [22]. The limiting factors are to a great extent regulated by upwelling, atmospheric deposition, ocean and mixed layer dynamics as well as solar cycles [23]. Net primary production is greatly influenced by wind-driven upwelling which brings nutrient-rich water from the deep ocean to the surface [24]. These coastal upwelling regions are usually found on the western side of the continent like West Africa where the Gulf of Guinea is located [18]. Globally, despite its occupying less than 1% area, these upwelling regions produce about 10% of primary production [25]. As a result of climate change, winds that favour the occurrence of upwelling have been projected to increase due to different rates of warming of land and ocean [25]. This is expected to lead to reduced SST in some parts of the world thereby increasing primary production in form of photosynthetic phytoplankton [26,27].

Photosynthetic phytoplankton are expected to be the fastest to be impacted due to their small size and fast rates of proliferation [28,29]. This is expected to lead to one of the most rapid impacts of climate change on the global marine ecosystem [30,31]. This is expected to be mostly in form of changes in rates and distribution of marine primary production which is expected to have both direct and indirect impacts on the global marine food web as diatoms, and fish and their associated predators are projected to decrease and the microbial food web to increase under global warming scenarios [32–34].

Due to the time-consuming, limited spatio-temporal coverage and expensive nature of the various methods used in the in-situ measurement of marine primary production, studies mostly rely on satellites remotely-sensed and ocean models data to assess the trends in this important ocean properties [3]. Studies such as [31,35] have employed the use of ecosystem models in assessing the impacts of climate change on the net primary production under different climate change scenarios and the uncertainties inherent in the estimation. Models from recent studies showed how climate change impacts lower trophic level organisms, and these effects are transferred through the food chain to larger animals which has societal impacts on fisheries [31,35]. These studies have found that

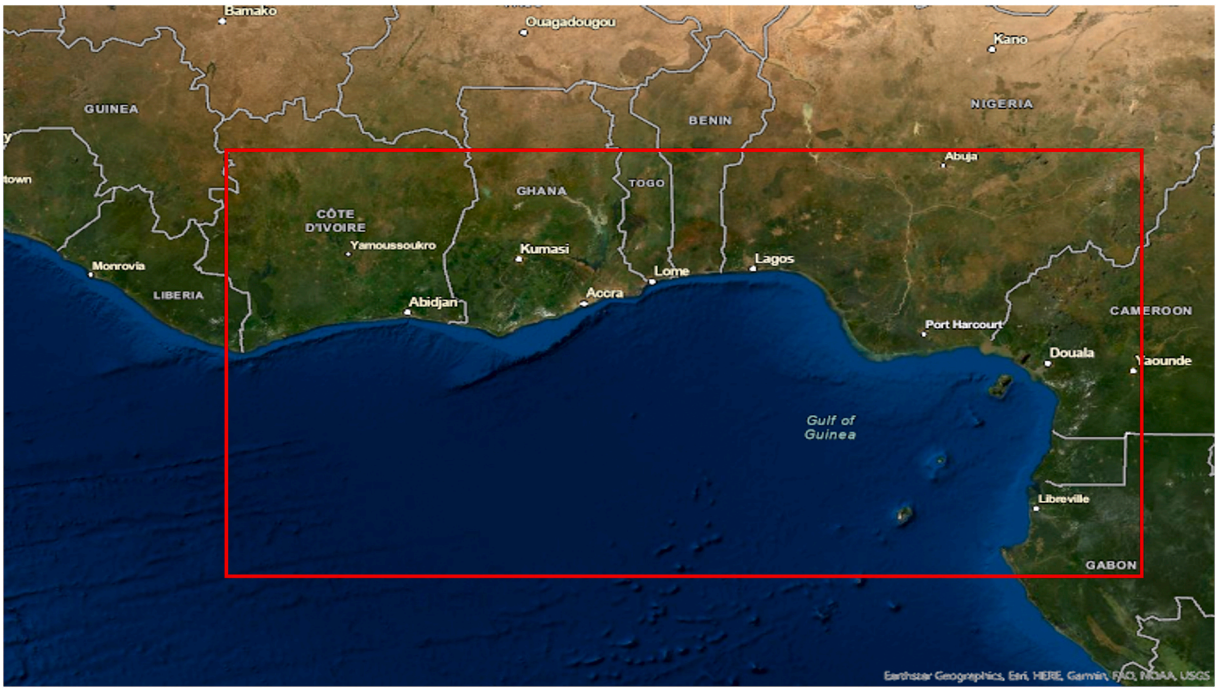

Fig. 1. Map of study area covering West African coastal waters including Gulf of Guinea (Red box shows the focus of the study)

Table 1
Summary of the data used in the study.

Data product	Global_reanalysis_bio_001_029	Global_analysis_forecast_bio_001_028	Global-reanalysis-phy-001-031	Global_analysis_forecast_phy_001_024
Acronym	GRB	GAB	GRP	GAP
Data Type	Model			
Acquisition Tool	NEMO PISCES biogeochemical model		Operational Mercator global ocean analysis and forecast system	
Water levels	Surface			
Temporal Coverage	1993–2018	2019–2020	1993–2018	2019–2020
Temporal Resolution	Daily			
Spatial Resolution	0.25° × 0.25°		0.083° × 0.083°	
Parameters acquired	Chlorophyll, Nitrate, Phosphate, Silicate, Dissolved Oxygen, Primary Production		Sea water potential temperature and Sea water salinity	
Source	https://data.marine.copernicus.eu/product/GLOBAL_MULTIYEAR_BGC_001_029/services	https://data.marine.copernicus.eu/product/GLOBAL_ANALYSIS_FORECAST_BIO_001_028/services	https://data.marine.copernicus.eu/product/GLOBAL_REANALYSIS_PHY_001_031/services	https://data.marine.copernicus.eu/product/GLOBAL_ANALYSISFORECAST_PHY_001_024/services
User Manual	https://catalogue.marine.copernicus.eu/documents/PUM/CMEMS-GLO-PUM-001-029.pdf	https://catalogue.marine.copernicus.eu/documents/PUM/CMEMS-GLO-PUM-001-028.pdf	https://catalogue.marine.copernicus.eu/documents/PUM/CMEMS-GLO-PUM-001-031.pdf	https://catalogue.marine.copernicus.eu/documents/PUM/CMEMS-GLO-PUM-001-024.pdf
Quality Information Document	https://catalogue.marine.copernicus.eu/documents/QUID/CMEMS-GLO-QUID-001-029.pdf	https://catalogue.marine.copernicus.eu/documents/QUID/CMEMS-GLO-QUID-001-028.pdf	https://catalogue.marine.copernicus.eu/documents/QUID/CMEMS-GLO-QUID-001-031.pdf	https://catalogue.marine.copernicus.eu/documents/QUID/CMEMS-GLO-QUID-001-024.pdf

change in water temperature can affect very important marine processes including rates of metabolic reaction causing molecular to ecosystem scale impacts [31]. The two most predominant forcings used in driving these models for projecting climate change impacts on the ecosystems are temperature and net primary production [36]. Other drivers which are used in place of the net primary production include phytoplankton and zooplankton biomass as well as export carbon.

Mostly, these studies are on global scale which provides the average condition on basin scale but not entirely representative of the regional situation in locations such as the GoG. Consequently, as a result of the importance in the role played by the primary production in the sustenance of the whole marine food web, the goal of this study is to make use of ocean model data in the assessment of the impacts of the changes in physical and biogeochemical parameters on the primary production of the Gulf of Guinea region. Model physical and biogeochemical data between 1993 and 2020 will be statistically analyzed to check their trends and possible impacts on the biological productivity of the GoG. The remaining part of this article is structured as follows. The study area in the Gulf of Guinea, data acquisition and data analyses methods are described in section 2. The results are presented and discussed in section 3 and the conclusion given in section 4.

2. Materials and methods

2.1. Study area

The focus of this study is the GoG, the coastal water of West Africa, located in the northern part of the Atlantic Ocean close to the equator. For this assessment, the coverage of the GoG is defined from Cape Palmas in Liberia down to Cape Lopez in Gabon including the island country of Sao Tome and Principe (red rectangular box in Fig. 1). This ranges between longitudes 15°E and 2.6°W and latitudes 10°N and 1.5°S. The GoG region is known to have relatively uniform oceanic conditions in terms of bathymetry, hydrography, productivity and trophic dynamics due to the predominant eastward flowing Guinea Current.

The GoG region has a strong upwelling between the coast of Cote d'Ivoire and Benin Republic popularly referred to as the Central West African Upwelling [37,38]. This very productive coastal upwelling system peaks between July and September with minor upwelling seasons between December and March [39,40]. This upwelling system is believed to be weakening as a result of the impact of climate change in the region since temperature is known to play a crucial role in the marine productivity of the GoG [41].

2.2. Data acquisition

For this study, the data source is the publicly available reanalysis data from the Copernicus Marine Environment Monitoring Service (CMEMS). The four globally available products used in this study are GLOBAL_REANALYSIS_BIO_001_029, GLOBAL-REANALYSIS-PHY-001-031, GLOBAL_ANALYSIS_FORECAST_PHY_001_024 and GLOBAL_ANALYSIS_FORECAST_BIO_001_028 which will henceforth be referred to as GRB, GRP, GAP and GAB respectively (Table 1).

Both GRP and GAP are multi-year 3D potential temperature, salinity and currents reanalysis and analysis forecast, respectively, from top to bottom. These global products contain the physical state variables of the ocean including seawater temperature (°C), seawater salinity (PSU), sea surface level/height (m), seawater velocity (ms^{-1}), mixed-layer thickness (m) but the daily mean of Sea Surface Salinity (SSS) and Sea Surface Temperature (SST) was used in this study. All the variables of the GAP are defined on the same standard grid of 1/12° which is approximately 8 km with 50 standard levels of which only the surface level is selected for this study [42]. While the GRP has a spatial resolution of 0.25° × 0.25° regular grid. The grid points in GRP and GAP that have the same longitudes and latitudes were extracted and concatenated.

Both GRP and GAP are improved with data assimilation using data from satellite and in-situ observations. The GRP contains four reanalyses namely GLORYS2V4 by Mercator Ocean (France), ORAS5 by European Centre for Medium Range Weather Forecast (ECMWF), GloSea5 by Met Office (UK) and C-GLORS05 by Centro Euro-Mediterraneo sui Cambiamenti Climatici (CMCC) (Italy) of which the ORAS5 was selected for this study. The GRP spans a period of 01-01-1993 to 31-12-2019 while the GAP covers the period of 01-01-2016 till date. The period 01-01-1993 to 31-12-2018 from GRP was merged with period 01-01-2019 to 31-12-2020 for this study. The daily version of both GAP and GRP were downloaded for this study.

GRB and GAB are also multi-year 3D hindcast biogeochemical products though the GRB has no data assimilation and the GAB has some data assimilation of ocean colour observation. Like the GRP and GAP, these globally available biogeochemical products are produced by Mercator-Ocean [43,44]. The daily product used in this study contains six variables vis-à-vis dissolved oxygen (DO) in mmol. m^{-3}, chlorophyll (Chl) in mg m^{-3}, net primary production (NPPV) in mg.m^{-3}.day^{-1}, silicate (Sil) in mmol. m^{-3}, nitrate (NO_3) in mmol. m^{-3} and phosphate (PO_4) in mmol. m^{-3} which are all used in this study. The temporal and spatial resolutions of GAB and GRB are also similar to that of GAP and GRP respectively.

According to a study by Varona et al. [45] on key atmospheric and oceanic parameters in the tropical Atlantic ocean where the GoG is located, these data can be adjudged useful. This is especially for scientists who want to embark on in-depth analyses to interpret trends of both physical and biogeochemical in the atmosphere and ocean in the tropical Atlantic Ocean. This is because they provide relevant data to research trends in ocean climate through statistical studies.

2.3. Trend analysis and significance test

The data analysis for the trend assessment done in this study was carried out by first averaging the daily data downloaded on a yearly basis for all the parameters considered. These yearly averages were then subjected to trend analysis using the linear regression

approach employed by the MATLAB climate toolbox function "trend" [46]. This works on the principle of finding the linear trend of a data series by least-squares method.

To confirm the significance of the changes observed in the trend analysis, the Mann Kendall test was also carried out. This was done using the "mann_kendall" function in the aforementioned toolbox. This works by giving an output of 1 if true i.e., the trend is statistically significant and zero if false when one can reject the hypothesis of the presence of a significant trend.

These analyses were done on an annual as well as a seasonal bases to explain the interannual and intersessional variations in the climate and biogeochemical parameters considered in this study. The seasonal analysis was done by separating the data into dry season months (winter) and rainy season months (summer). Winter was defined similar to those used in previous studies by Dahunsi et al. [38] in the GoG as months from November to March. Summer starts from April to October which is the major rainy season for the GoG region.

2.4. Determination of drivers of primary production

In order to determine the potential drivers of primary productivity in the GoG, principal component analysis (PCA) was carried out on the nutrient and physico-chemical parameters: NPPV, Chl, DO, NO_3, PO_4, Sil, SSS and SST. These parameters were averaged spatially (in the longitude and latitude dimension) to give 1-deminaional daily data between January 1993–December 2020. These aforementioned variables were de-meaned to reduce bias resulting from differences in variables magnitude and measuring units. After this, the "PCA" function of MATLAB was applied to determine the principal components coefficients and Eigen-values. This method centres the datasets containing all the variables of interest in different columns before applying the singular value decomposition algorithm on it. It also allows the estimation of the percentage (%) of the total variance in the dataset explained by each principal component. To explain the relationships between the various parameters, correlation analysis was also done. These are presented in the results and discussion section.

3. Results and discussion

3.1. Sea surface temperature (SST)

Generally, both the spatial and temporal trend analyses done show that the SST in the GoG has been experiencing increase between 1993 and 2020. Close to the coast, this increasing trend is higher off the coast of Benin Republic in West Africa, off Cameroon and the

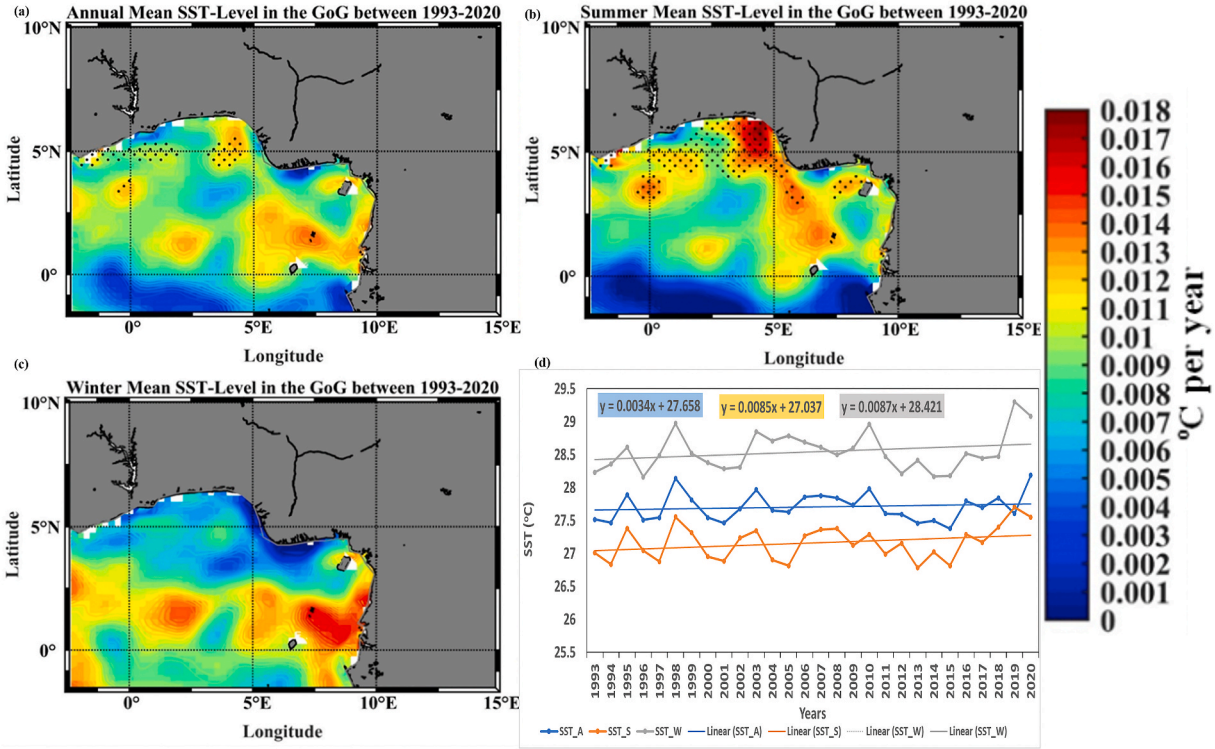

Fig. 2. Spatial trend of average Sea Surface Temperature in the GoG between 1993 and 2020 (black dots show regions with significant trend) (a) Annual (b) Summer (c) Winter (d) Temporal on annual (SST_A), summer (SST_S) and winter (SST_W) bases with their corresponding linear regression lines.

adjacent islands of Sao Tome and Principe as well as the southern coast of the GoG as seen in the spatial maps in Fig. 2a–c. The average SST in the GoG was estimated as 27.7° and positive trends generally higher than 0.012 °C per year are observed in these regions. The south eastern part of Nigeria around the Niger Delta shows a very low rate of increase of about 0.001–0.004 °C per year. This round the year increasing SST depicts that the impacts of climate change are being witness in the surface water of the GoG.

The inter-seasonal variations in SST trends can be observed when Fig. 2b and c are compared. It can be seen that higher increasing trends are seen closer to the coast during the summer while the reverse is the case during the winter. The Mann-Kendal trend significance test done showed that the trends are significant in more places in the summer than in the winter as shown by the black dots on the trend maps. It can be deduced that a significant increase has been experienced in the SST on the coastal strip of the GoG during the summer between 1993 and 2020. This seem not to hold for the regions with major rivers like the Volta and Niger as these regions have different trends which could not be statistically classified as significant.

In a study assessing the trends in SST and Chl in the major Large Marine Ecosystems in Africa [47], found the GoG is the third fastest warming of all the seven ecosystems studied. Similar to what can be seen on Fig. 2a–c which shows that all parts of the GoG have been experiencing warming [47], reported 100% warming in the region too. The study also captured the hotspot of increase seen off the Benin Republic-Nigerian coast which is more obvious in Fig. 2b.

Fig. 2d confirms that higher SST are experienced during the dry season (winter) with SST generally higher than 28 °C whereas the rainy season (summer) has SST less than 28 °C. The general trend shows that the rate of increase in the winter is higher than in summer with values of 0.0087 and 0.0085 °C per year respectively. This increase can be observed to have been continuous between 2015 and 2020. In a study assessing the relationships between SST and primary production by Chiswell and Sutton [48], they found SST increase up to 0.7 °C per decade in the New Zealand region.

Li et al. [49] suggested that the increase in mean temperature which can partly be attributed to climate change will impact the mixed layer depth through its effect on thermal stratification. This is in fact due to the ocean-atmosphere interaction in terms of exchange of mass, energy and momentum through physical processes. Research has proved that there exists a positive correlation between SST and precipitation [23]. The Nigerian coast which was observed to be the warmest by Ayinde et al. [23] is seen to be the region with the least increasing trend in SST owing to its already warm coastal water.

3.2. Sea surface salinity (SSS)

Unlike the SST trend which has been generally increasing, regions of decreasing SSS can be seen on the spatial distribution of trends in Fig. 3a–c. This is obvious from Cameroon southward on the annual and seasonal trend spatial distribution maps. Close to the coast

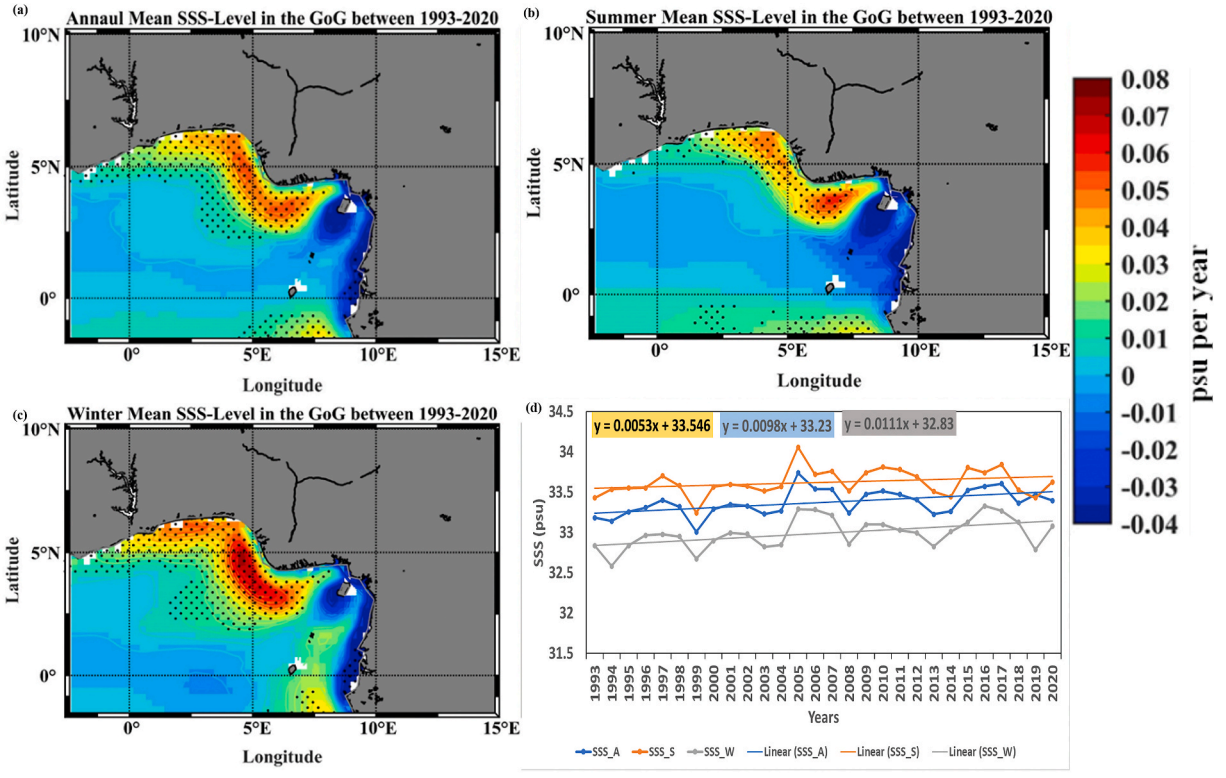

Fig. 3. Spatial trend of average Sea Surface Salinity in the GoG between 1993 and 2020 (black dots show regions with significant trend) (a) Annual (b) Summer (c) Winter (d) Temporal on annual (SSS_A), summer (SSS_S) and winter (SSS_W) bases with their corresponding linear regression lines.

from Ghana to Nigeria, it can be seen that the SSS has been increasing at higher rates up to 0.08 psu per year in some cases. This trend is round the year though it can be seen to be stronger in the dry season which suggests that temperature plays major role in the changes of the SSS in the GoG. This deduction can be strengthened when the trend during the summer which is the major upwelling season is observed. Coastal upwelling seems not to be the major influence in the increasing SSS in the GoG because even the eastern regions with weaker upwelling have been experiencing higher rates of increasing SSS especially off the Nigerian coast.

The black dots (Mann-Kendal test) around the coast show that the increase in SSS close to the coast between 1993 and 2020 has been significant. Though SSS is generally higher during the summer than in winter, as seen in Fig. 3d, the linear regression line confirmed a higher rate of increase of 0.0111 psu per year for the winter than the 0.0053 psu per year in summer. Also, contrary to the continuous increase from 2015 to 2020 seen in SST, the reverse seems to be the case for SSS. This confirms that temperature alone is not the determinant of the SSS of a region as other factor like rainfall and river discharge play major roles [50]. Curry et al. [51] also found that atmospheric freshwater fluxes contributed to the change in SSS.

From the time series plot in Fig. 3d, it can be observed that the SSS in the GoG has an oscillating cycle which usually last for five years before another cycle. This cycle is noticed in both the annual plots and seasonal graphs. This cycle results into several years of relatively high peaks as seen in 2005 and 2010 and distinct lows like 1994, 1999, 2008, 2013 and 2019.

Increase in salinity in the Gulf of Guinea had previously been reported by Houndegnonto et al. [52] but with magnitude smaller than the period under this study. They also noted a decadal variability in SSS in addition to an increasing salinity trend in this region. Interestingly, a global analysis also suggested that some of the largest increases in SSS over the period 1950–2008 were found in the Gulf of Guinea [53–55]. However Da-Allada et al. [53], suggested that the increasing trend may have been a part of a more complex processes.

3.3. Chlorophyll-A (Chl)

The spatial distributions of trends in Fig. 4a–c shows that the chlorophyl-A level in the GoG has been experiencing increase in almost every part. This increasing trend does not vary with season though it can be seen that the rate of increase is higher during the summer in the whole of the GoG. These higher rates in the summer can be linked to the coincidence with the major upwelling season in the GoG region, that is, the boreal summer upwelling phenomenon at Cote d'Ivoire and Ghana coasts [23]. This deduction can be strengthened by looking at the rates of increase in the major upwelling north-western coastal area of the GoG between Cote d'Ivoire and Benin Republic. The general spatial trend indicates an increase in the concentration of chlorophyll-A from the coast to the open sea and a decrease from the Liberian coast to the Nigerian coast [23]. This stronger coastal upwelling region showed higher rates of increasing concentration of chlorophyll-A between 1993 and 2020. The representation of the Mann-Kendal trend significance test i.e.,

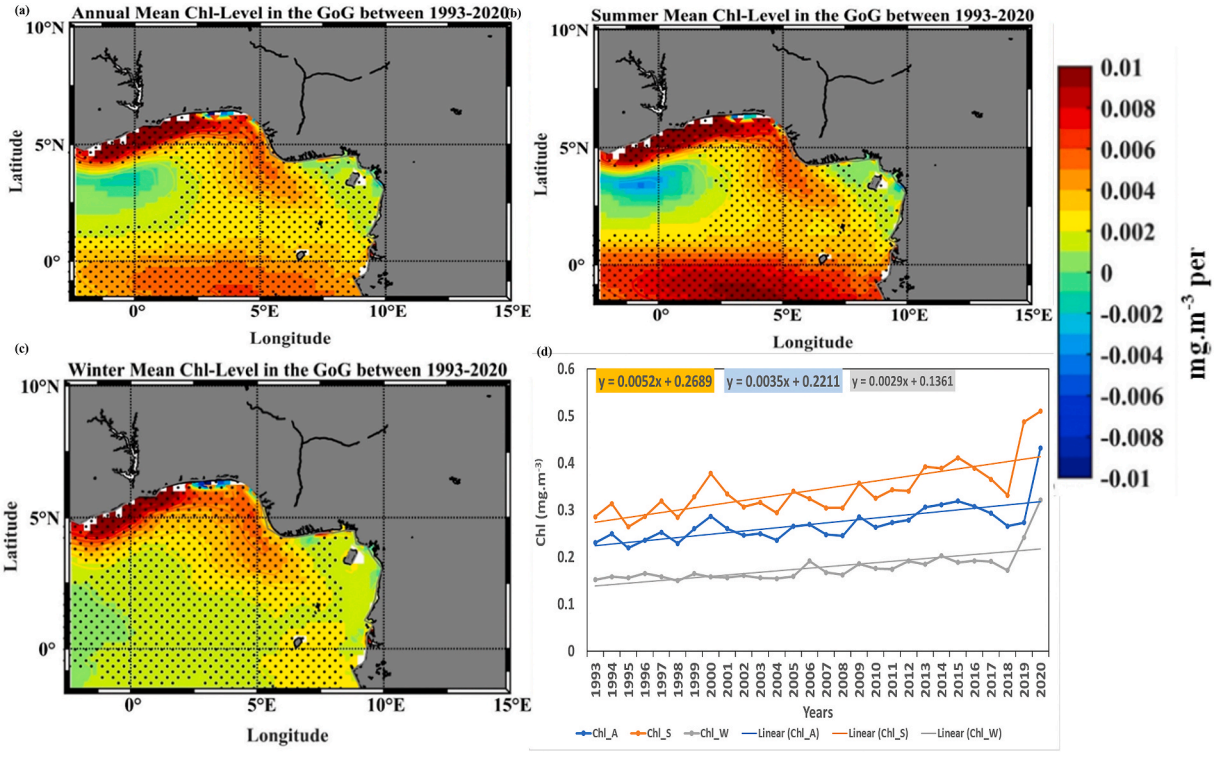

Fig. 4. Spatial trend of average Chlorophyl-A level in the GoG between 1993 and 2020 (black dots show regions with significant trend) (a) Annual (b) Summer (c) Winter (d) Temporal on annual (Chl_A), summer (Chl_S) and winter (Chl_W) bases with their corresponding linear regression lines.

the black dots show that the changes in chlorophyll-A experienced in the GoG can be adjudged as statistically significant between 1993 and 2020. The higher rates of increase seen in the summer which is the major raining season in the GoG can also be the explanation for the fact that chlorophyll-A is increasing despite increasing SST. Increased rainfall due to climate change is expected to increase river discharge and hence the supply of some nutrients from land sources.

Fig. 4d confirms results showing higher values for chlorophyll-A concentration reported in previous studies for most part of the GoG. The maximum value of chlorophyll-A concentration which is seen in 2020 is about 0.5 and 0.3 mg m^{-3} for the summer and winter season respectively. On average, the chlorophyll-A concentration in the GoG has been increasing by 0.0035 mg m^{-3} per year on an annual basis while rates of 0.0029 and 0.0052 mg m^{-3} per year was estimated for the dry and rainy season respectively. This results are similar to the findings of Sweijd and Smit [47] where a median Chl value of 0.23 and ranging from 0.14 to 5.14 mg/m^3 was reported. Chiswell and Sutton [48] found chlorophyl increase of about 0.04 mg/m^3 per decade which is comparable when converted to the yearly increase repoted in this study.

On average, a one-year cycle of maximum and minimum can be observed to be oscillating in the timeseries plot in Fig. 4d. An observation of good correlations can be seen when the timeseries plots of SST, SSS and Chl are compared. This deduction was drawn from years with low SST and high SSS coinciding with years with higher concentration of Chl. For example, years 2005 with an exception in 2020 which has the highest Chl despite not satisfying the condition of low SST. The observed increase in Chl concentration can be attributed to upwelling. This was in agreement with findings of Nieto and Mélin [18] who suggested that upwelling conditions with cold SST, negative sea level anomalies (SLA), fairly strong frontal activity, and moderate winds, appeared as the environmental window most favourable to high Chl values amongst other mixed properties.

Similar to the findings in this study, it is important to note that net primary production or chlorophyll-A has an inverse relationship with SST as it is known that high SST depletes Dissolved Oxygen (DO) in the ocean [23]. This may not be the case in some scenarios, for example, the year 2020 has the highest Chl and does not satisfy the condition of low SST. The Nigerian coast already known for its low chlorophyl-A concentration as mentioned by Ayinde et al. [23] is also among the regions with least increasing trend in Chl because of the warm nature of the water.

The years of exception to the negative correlation known between SST and Chl became more obvious from 2018. This is expected to be a result of one of the factors contributing to primary production overshadowing the impacts of SST in the GoG. According to the findings of Martins and Stammer [56], the year 2018 marks the strong influence of Congo River in the southern part of the GoG. According to Martins and Stammer [56], the year 2019 has the strongest river discharge in the last 4 decades as a result of anomalous high precipitation in the over the African continent. This is expected to strengthen the supply of nutrient from river discharge leading

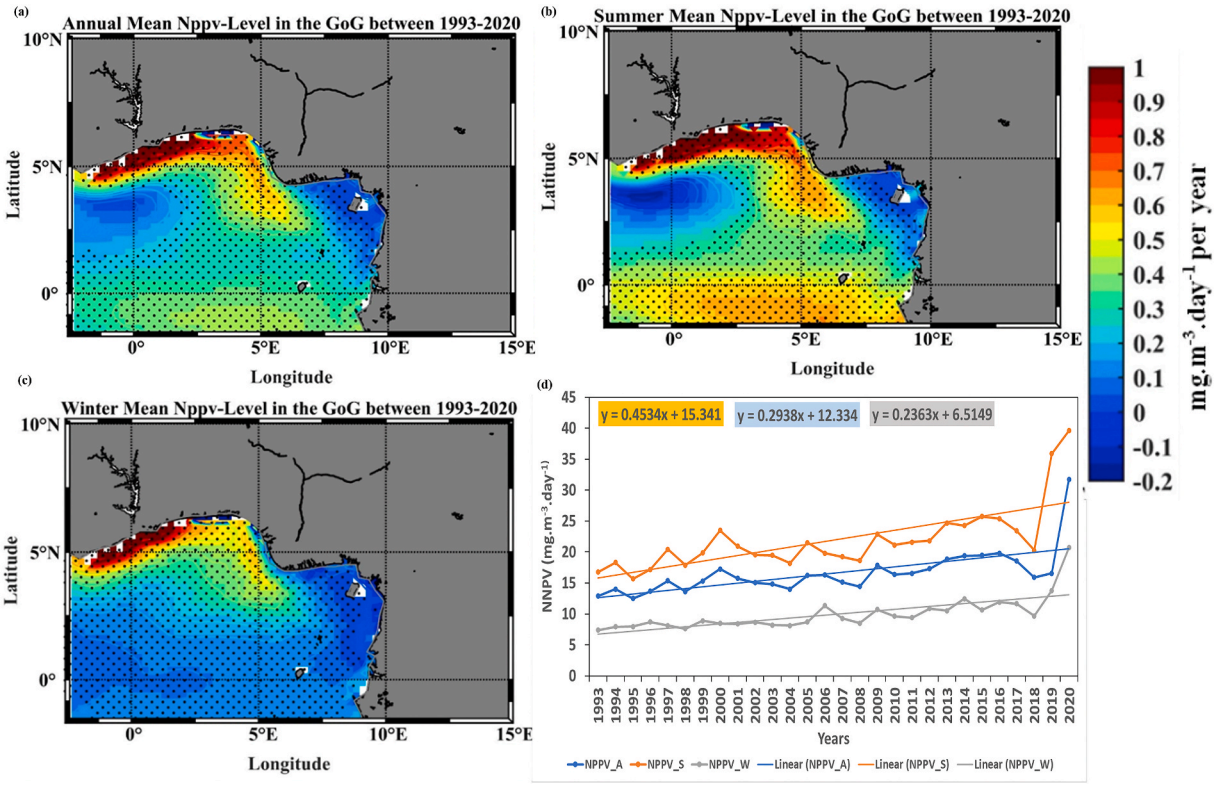

Fig. 5. Spatial trend of average Net Primary Production level in the GoG between 1993 and 2020 (black dots show regions with significant trend) (a) Annual (b) Summer (c) Winter (d) Temporal on annual (NPPV_A), summer (NPPV_S) and winter (NPPV_W) bases with their corresponding linear regression lines.

to the highest Chl seen in 2020.

3.4. Net primary production (NPPV)

Fig. 5a–c shows very similar spatial distribution to that seen in the previous section on chlorophyl-A concentration. Though the trend values are some orders of magnitudes higher than seen for Chl, the net primary production in the GoG has been experiencing an increase in some parts of the GoG. This increase is obvious in the coastal parts of the north-western part of the GoG with stronger upwelling. The Mann-Kendall test showed that these trends are statistically significant in most of the GoG round the year. Very little increase and in some cases, a decrease has been seen in the eastern parts of the GoG especially off the coast of Nigeria. This insignificant decrease is also seen offshore around Cote d'Ivoire-Ghana region which was also captured as the region with the weakest increase in Chl between the study period. Another very interesting observation seen in Fig. 5a–c, which is also observed in the spatial distribution of the trends for Chl, is the uniqueness and similarity between the equatorial upwelling region around latitude 0 and the coastal upwelling region in the north-western part of Cote d'Ivoire-Benin Republic and also the south-eastern part around off Equatorial Guinea-Gabon axis. Though the values are less during the winter, it can still be seen that the increasing trend in this equatorial upwelling region was still captured.

Again, comparing the seasonal spatial distribution of the trends, a level of intersessional variation can be observed. This is in form of high NPPV in the summer than in winter. Fig. 5d confirms this seasonal variability with values of NPPV averaging about 40 mg m^{-3}. day^{-1} in the summer while the maximum value seen in 2020 for the dry season is half that of the summer.

Similar to the previously reported yearly rise and fall of the Chl, the case of the NPPV is also very similar. The trend on annual basis estimated for the GoG is 0.2938 mg m^{-3}.day^{-1} per year while the values are 0.4534 *and* 0.2363 mg m^{-3}.day^{-1} per year for summer and winter, respectively. The study by Sweijd and Smit [47] also confirmed the positive trend of NPPV in the GoG. This same trend was found for all the major marine ecosystems in the western part of Africa.

The variabilities observed in this study have been identified by previous studies which have also showed that marine fisheries production is primarily governed by available primary production [11,57]. Additionally, changes in primary production [11] and temperature [31] affected growth rates and fish production, altering the responses of ecosystems to fishing.

3.5. Nitrate (NO_3)

The spatial distributions of the pattern of changes seen in the Nitrate level in the GoG are presented in Fig. 6a–c. Generally, in the

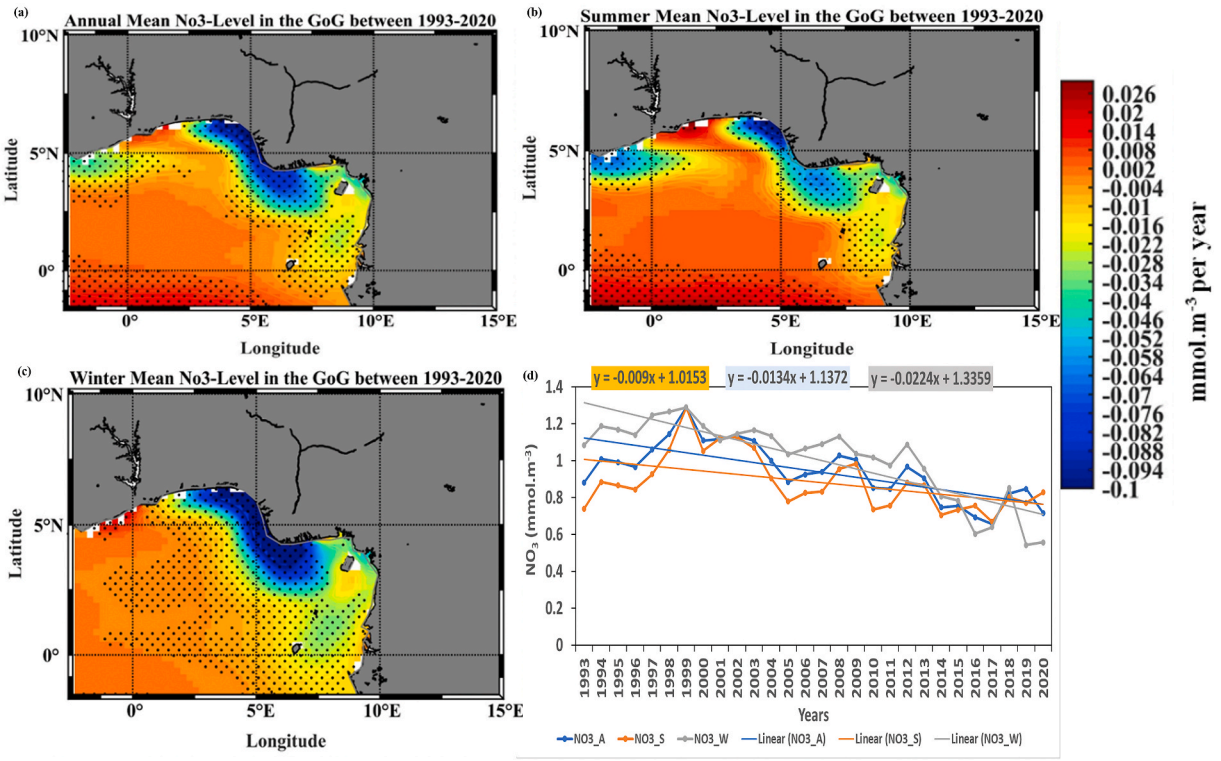

Fig. 6. Spatial trend of average Nitrate level in the GoG between 1993 and 2020 (black dots show regions with significant trend) (a) Annual (b) Summer (c) Winter (d) Temporal on annual (NO3_A), summer (NO3_S) and winter (NO3_W) bases with their corresponding linear regression lines.

coastal areas of the GoG, the NO_3 has been experiencing a decreasing trend between 1993 and 2020. The only exception to this decreasing trend is the region surrounding the entry point of the Volta River into the Atlantic Ocean which shows a positive trend. This distinct region is seen on both the annual and summer spatial distribution but a westward extension of this increasing trend is seen during the winter. This is evidenced in the positive trends seen around the coastal areas of Cote d'Ivoire to Togo during the dry season. Nevertheless, positive trends are observed round the year offshore. This positive trend is especially strong in the coastal and equatorial upwelling region which suggests that upwelling is a major contributing factor to the abundance of NO_3 in the GoG region. The intensity of the offshore increase is also higher during the summer which is the major upwelling season in the region [58]. A negative trend is seen around the coast of Nigeria down to Cameroon despite the presence of major rivers as well as the Niger Delta emphasizing the predominance of upwelling over the river supply from land in NO_3 distribution. The black dots representing the Mann Kendal test on Fig. 6a–c showed that both the negative and positive trends are statistically significant round the year in the coastal areas as well as the equatorial upwelling region.

Negative trends of −0.0134, −0.009 and −0.0224 mmol m^{-3} per year have been estimated on an annual, summer and winner basis, respectively for the GoG between 1993 and 2020 as shown by the linear trend lines in Fig. 5d. Similar to the high concentration of NO_3 reported for the winter with values higher than 1.2 mmol m^{-3} in 2009, it can be seen that the concentration of NO_3 in the GoG has been declining at a faster rate than during the rainy season. Contrary to the maximum NPPV and Chl reported in the year 2020, the NO_3 concentration for 2020 happens to be one of the least during the study period. This suggests that other factors played major role in the chlorophyll-A concentration and net primary production level reported for 2020. Citing the report by EPA [59], Ayinde et al. [23] mentioned that the low nitrate level seen in 2009 and 2014 can be linked to the reduction in the use of nitrogen as a major fertilizer applied in the agriculture. This is expected to lead to reduce land-sea deposition of nitrate through run-off from farmlands.

3.6. Phosphate (PO_4)

Similar to what was seen in the spatial distribution of NO_3 trend, Fig. 7a–c shows that the trends of PO_4 are higher in the coastal and equatorial upwelling regions. This is especially obvious off the coast of Ghana–Benin Republic where increasing trends as high as 0.0058 mmol m^{-3} per year can be seen. This region of increasing trend is more distinct and extends farther offshore during the rainy season (Fig. 7b) than the winter (Fig. 7c). Though mostly positive for PO_4, the trends reported for PO_4 are one order of magnitude less than the generally negative trends for NO_3. Also, similar to the case of NO_3, the trends of PO_4 in the eastern part of the GoG especially off the coast of Nigeria-Cameroon show decreasing trends. The significance of trend test showed statistically significant trend in most parts round the year as depicted by the black dots representing the Mann Kendal test on Fig. 7a–c. An exception is seen for the region

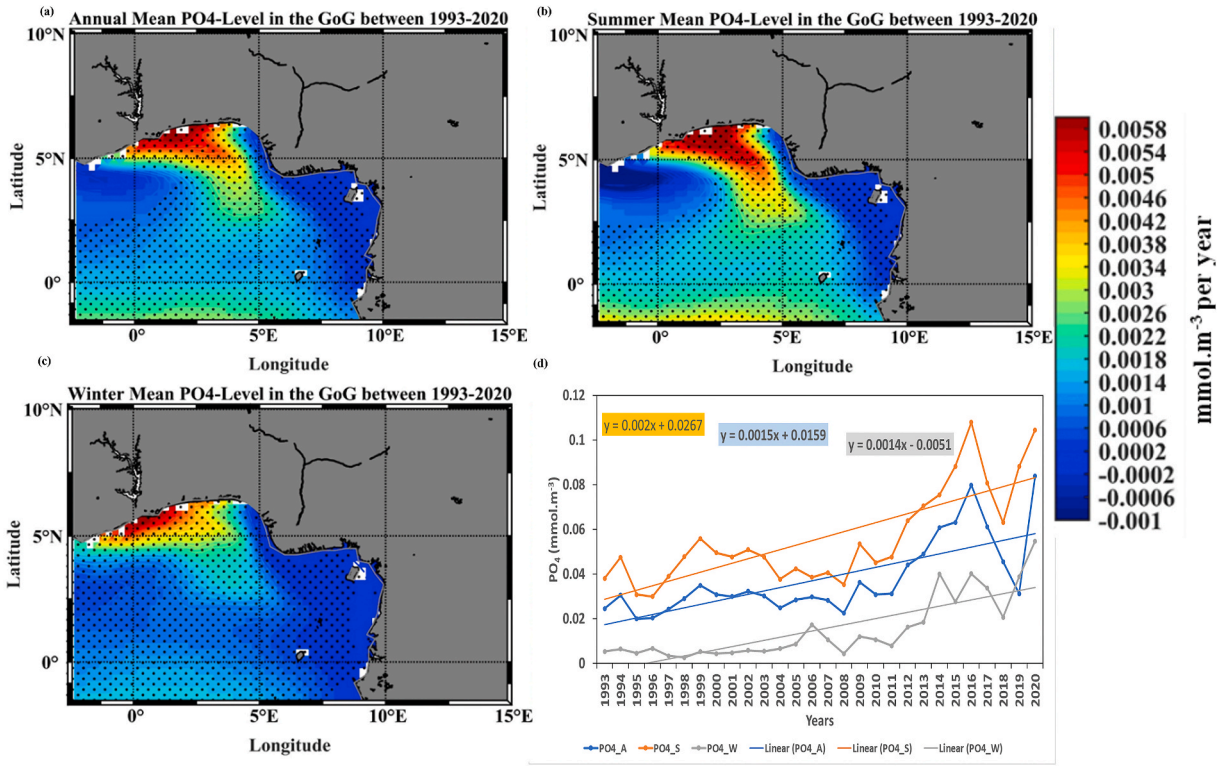

Fig. 7. Spatial trend of average Phosphate level in the GoG between 1993 and 2020 (black dots show regions with significant trend) (a) Annual (b) Summer (c) Winter (d) Temporal on annual (PO4_A), summer (PO4_S) and winter (PO4_W) bases with their corresponding linear regression lines.

offshore Cote d'Ivoire-Ghana with a distinct trend for almost all the parameters considered in this study. This region located approximately between 5°N–2.5°N and 0–1.6°W has been observed to have a different pattern from the surrounding areas to the east and south in most instances.

Fig. 7d showed that higher concentrations of PO_4 are recorded during the rainy season than winter in the GoG contrary to what was seen for NO_3. Concentrations higher than 0.1 mmol m^{-3} was seen for peak years 2016 and 2020 during the summer. It is noteworthy that one of the highest concentrations of PO_4 is reported for the year 2020 which has been previously seen as the most productive year in terms of Chl and NPPV. The westward advection of the anomalous events found by Martins and Stammer [56] and contribution of large rivers such as Niger and Volta Rivers are the plausible explanation for the increased nutrients supply to coastal waters observed from 2018. This was affirmed in a study by Auricht et al. [60] where a corelation greater than 0.6 was found between the Niger River discharge and Chl for he GoG. This high correlation was found despite many months of missing data for river discharge which is one of the factors inhibiting studies requiring long temporal data in the GoG. The average PO_4 trend values for the GoG between 1993 and 2020 are estimated as 0.0015, 0.002 and 0.0014 mmol m^{-3} per year on an annual, summer and winter basis respectively. It can be observed that between 2011 and 2016, a continuously increasing concentration of PO_4 has been recorded in the GoG until two years of decline between 2017 and 2018 after which the concentration has also been on a continuous increase.

3.7. Silicate (Sil)

From the spatial distribution of the trends in the silicate concentration in the GoG between 1993 and 2020 presented in Fig. 8a–c, it can be observed that on average, most places have been experiencing decline in silicate concentration. This decline is extreme in the eastern part of the GoG off Nigeria and Cameroon where deceasing rates as high as 0.3 mmol m^{-3} per year can be seen. Comparing Fig. 8b and c shows that the decrease in silicate concentration is at higher rates in the winter than in the summer. The only region with a seeming increasing trend of silicate concentration is the previously identified distinct region of the coast of Cote d'Ivoire to Ghana. The Mann-Kendal test done also showed that this basin-wide decreasing trend is statistically significant for a greater part of the GoG regions as can be seen by the black dots almost everywhere on the spatial distributions of trends for annual and seasonal analyses.

Fig. 8d shows that silicate follows a similar temporal trend with NO_3 because it can be observed that the concentration during the winter (dry season) is higher than in the rainy season. The winter has values generally higher than 5 mmol m^{-3} with a peak of about 5.5 mmol m^{-3} in 1998 whereas the concentration of silicate in the GoG is generally less than 5 mmol m^{-3} in the summer. The trends also follow the similar a pattern with values of -0.047, −0.0528 *and* −0.0649 mmol m^{-3} per year for annual, summer and winter average trends, respectively. Also contrary to phosphate which happens to be the only nutrients with values supporting the peak Chl

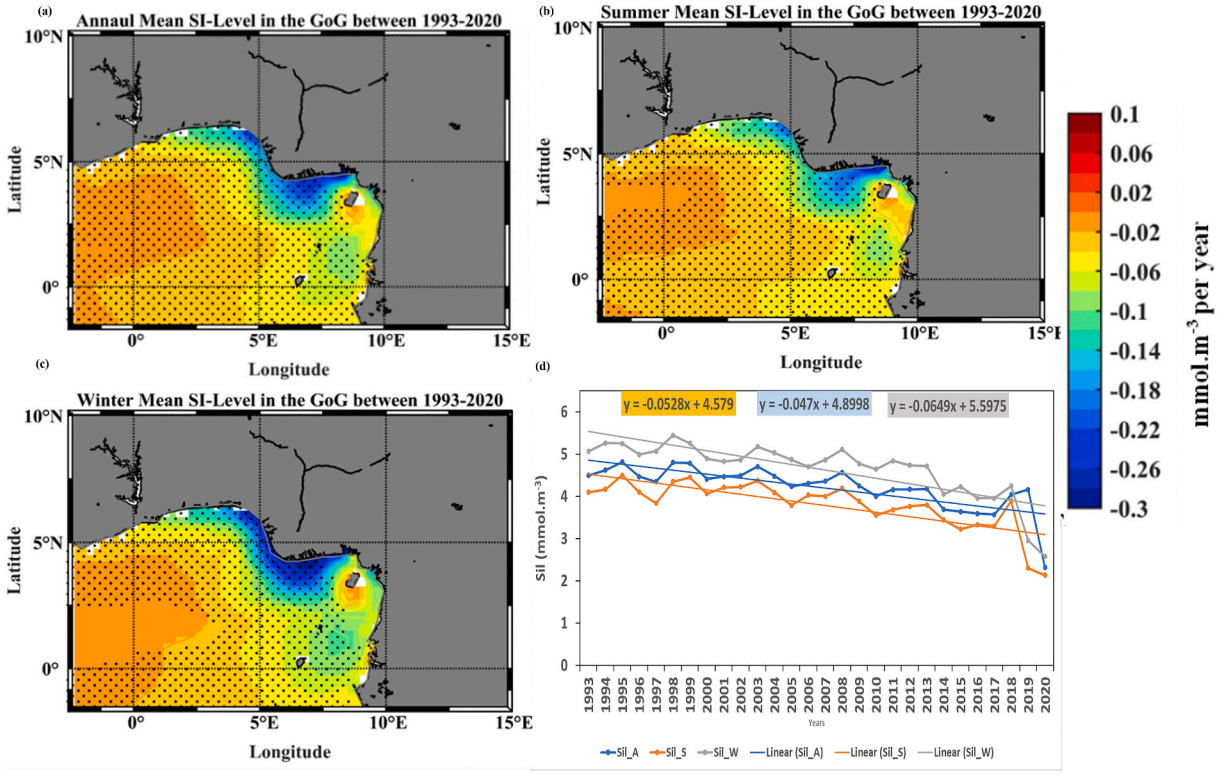

Fig. 8. Spatial trend of average Silicate level in the GoG between 1993 and 2020 (black dots show regions with significant trend) (a) Annual (b) Summer (c) Winter (d) Temporal on annual (Sil_A), summer (Sil_S) and winter (Sil_W) bases with their corresponding linear regression lines.

and NPPV values seen in 2020, the value of silicate concentration is the lowest just like that seen for NO_3. Though the trend of silicate is an order of magnitude higher than that of NO_3, the spatio-temporal analyses for both parameters show very similar patterns. The values reported for all the nutrients considered in this study are similar to the findings of Nubi et al. [61] that reported higher concentration of silicates than phosphate and nitrate in the coastal water of the GoG. The reduction of NO_3 found in this study is a cause for concern owing to the fact that primary production in the coastal waters of the GoG is limited by availability of NO_3 [62].

3.8. Dissolved oxygen (DO)

The spatial distribution of the trends of the Dissolved Oxygen in the GoG between 1993 and 2020 presented in Fig. 9a–c shows very similar patterns to those of PO_4 previously presented. An increasing trend of DO is seen in most parts of the GoG with higher values seen from Togo down to the southwestern part of Nigeria. The exceptions are seen in the previously identified distinct region offshore Cote d'Ivoire to Ghana and the south-eastern part of Nigeria through the coastal areas southward where negative trends can be observed. These regions of negative trends can be seen to have higher rates of change in the summer. The negative trend seen in the distinct region offshore Cote d'Ivoire to Ghana disappeared during the winter and the positive trends extended farther offshore towards Sao Tome and Principe. The Mann Kendal test showed that the changes experienced by DO in the GoG between 1993 and 2020 is only significant in few places notably the increasing trend region off Togo-Nigeria and the negative trend region off Cote d'Ivoire to Ghana.

The timeseries of DO between 1993 and 2020 for the GoG presented in Fig. 9d show that the DO concentration in the summer is higher than in the dry season. This is seen in a value of about 212 mmol m^{-3} recorded for the year 2013 in summer whereas the winter concentration is mostly less than 209 mmol m^{-3}. Despite these higher values in the rainy season, values of 0.0214, 0.0128 and 0.0159 mmol m^{-3} per year for annual, summer and winter trends depict a higher rate of increase in the DO during the winter. It is also worthy of note that there is a continuous rise and fall of the DO concentration oscillating every 1–3 years throughout the study period. A value that ranks among the highest is also recorded for the year 2020 which supports the previously reported high values of Chl and NPPV in the same year.

Out of all the nutrients considered in this study, only phosphate seems to correlate with the maximum productivity in terms of Chl and NPPV observed in 2020, therefore, being the most plausible driving factor despite unfavourable climatic factors like SST.

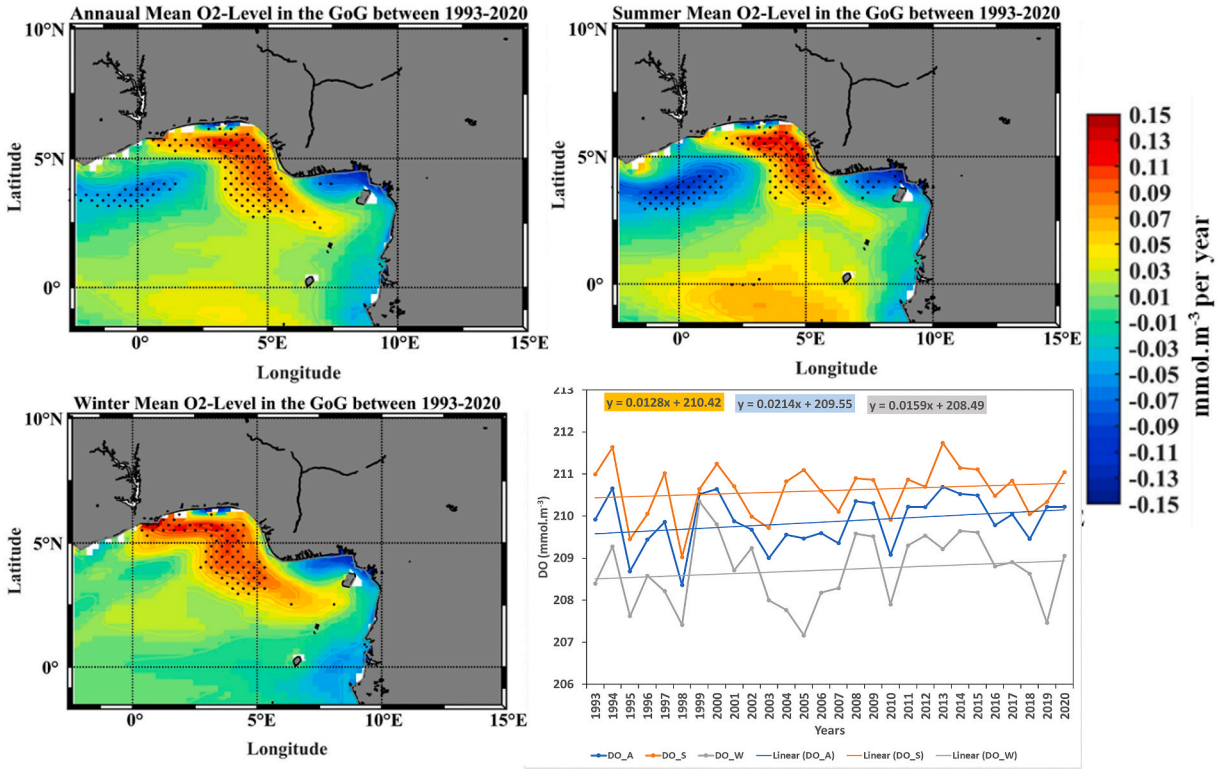

Fig. 9. Spatial trend of average Dissolved Oxygen level in the GoG between 1993 and 2020 (black dots show regions with significant trend) (a) Annual (b) Summer (c) Winter (d) Temporal on annual (DO_A), summer (DO_S) and winter (DO_W) bases with their corresponding linear regression lines.

3.9. Principal drivers of primary production

The results of the PCA test (Table 2) showed that the principal components are the first three (PC1, PC2 and PC3). These components explained a total of 99.1% of the variation in the dataset. Looking closely at the table, one can observe that each of these components have one predominant driving variables which are DO, Sil and SST for PC1, PC2 and PC3, respectively. This shows the influence of SST which has a strong negative effect on the first principal component, DO, as can be seen in the correlation presented in Table 3. A correlation of −0.90 between DO and SST shows a strong negative relationship which is expected to also result in negative impacts of climate change in the GoG. This suggests that continuous increasing SST will have a very negative impact on the primary productivity in the GoG since 90% of the variation in that NNPV is associated with DO. However, the results previously presented for the various parameters considered in this study showed that DO has been increasing despite increasing SST. This suggests that the increasing rate of SST in the GoG is not yet strong enough for the expected negative impacts on the DO. Another possible explanation of this contradiction is the impacts of increasing supply of nutrients overshadowing the effects of increased SST. This can be attributed to increased rainfall resulting in higher river discharge into the coastal waters of the GoG [23,63].

A closer observation of the correlation results coupled with previously presented findings gives an interesting insight into the driving factors of primary production in the GoG. With the knowledge that silicate is the second principal component after DO, the inter-relationship of Sil with other parameters showed that it has a fairly strong positive relation with SST. This means increasing SST is expected to translate to increase in Silicate but a look at the trend in Fig. 8d showed that silicate has been reducing in the GoG. The other nutrient (NO_3) which has a weak positive correlation with SST also showed reducing trend as seen in Fig. 6d. These results when coupled with the knowledge that silicate has very strong negative corelations of −0.82 and −0.78 with NPPV and Chl respectively confirmed that the supply of these nutrients to the water of the GoG currently overshadows the impacts of SST. Though in the future, higher increasing rates of SST may favour more silicates in the coastal waters of the GoG, it may not immediately translate to increase productivity as seen in the negative correlations, −0.77 and −0.80, of SST with NNPV and Chl, respectively. This may be due to negative relationship (−0.74) of SST with another important nutrient like PO_4. Similar to the case reported in this study Kadiri et al. [64], found a negative correlation between NO_3 and Silicate in the Nigerian arm of the GoG.

4. Conclusion

The trend analyses done in this study has shown that despite the increasing trend of SST as a result of climate change, the productivity indicators used i.e., Chl and NPPV also show that primary productivity of the GoG is also rising. The interplay between nutrients supplies through river discharge and other ocean circulation processes such as advection have been concluded to be the strongest explanation for this weak impacts of increasing SST in the GoG. This is expected to also translate to higher fish catch and benefits the increase in the abundance of other endangered marine organisms including sharks and turtles. Nevertheless, the risk of negative impacts of climate change on the whole ecosystem productivity cannot be categorically ruled out since community composition analysis was not done in this study. Therefore, it is recommended that future study which makes use of regional models that can simulate more complex predation and competition interaction within the GoG ecosystem be carried out. This will provide ecosystem managers the needed information to ascertain the species that are most at risk due to climate change.

Author contribution statement

Adeola M. Dahunsi: Conceived and designed the experiments; Performed the experiments; Analyzed and interpreted the data; Wrote the paper.

Tolulope S. Oyikeke, Mujeeb A. Abdulfatai & Lateef A. Afolabi: Performed the experiments; Analyzed and interpreted the data; Wrote the paper.

Funding statement

This research did not receive any specific grant from funding agencies in the public, commercial, or not-for-profit sectors.

Table 2
Summary of PCA output.

Parameters	PC1	PC2	PC3	PC4	PC5	PC6
DO	**0.91**	0.27	0.31	0.098	0.036	−0.00015
NO_3	−0.0028	0.16	−0.13	−0.34	**0.91**	−0.06
PO_4	0.0091	−0.025	−0.0021	−0.029	0.059	**0.99**
Sil	−0.15	**0.85**	−0.39	0.30	−0.097	0.036
SSS	0.095	−0.35	−0.27	**0.83**	0.33	−0.0063
SST	−0.39	0.22	**0.81**	0.32	0.20	0.008
Percentage	**90.0**	**6.67**	**2.43**	0.50	0.39	0.0019
Eigenvalue	10.87	0.81	0.29	0.06	0.047	0.00023

Table 3
Correlations between the variables assessed.

	NPPV	*Chl*	*DO*	*NO3*	*PO4*	*Sil*	*SSS*	*SST*
NPPV	1							
Chl	**0.98**	1						
DO	**0.70**	**0.70**	1					
NO3	−0.075	−0.057	−0.0044	1				
PO4	**0.91**	**0.90**	**0.65**	−0.028	1			
Sil	**−0.82**	**−0.78**	−0.48	0.48	**−0.81**	1		
SSS	**0.75**	**0.75**	**0.54**	−0.30	**0.73**	**−0.73**	1	
SST	**−0.77**	**−0.80**	**−0.90**	0.028	**−0.74**	**0.54**	**−0.72**	1

Data availability statement

Data associated with this study has been deposited at The data used are publy available data provided by Copernicus Marine Service.

It can be found here: https://resources.marine.copernicus.eu/products

Declaration of interest's statement

The authors declare no competing interests.

Acknowledgements

The authors are grateful to the Copernicus Marine Environment Monitoring Service (CMEMS) for making the data used for this study publicly available.

References

[1] F. Mattei, M. Scardi, Collection and analysis of a global marine phytoplankton primary-production dataset, Earth Syst. Sci. Data 13 (10) (2021) 4967–4985, https://doi.org/10.5194/essd-13-4967-2021.
[2] M.C. Carvalho, K.G. Schulz, B.D. Eyre, Respiration of new and old carbon in the surface ocean: implications for estimates of global oceanic gross primary productivity, Global Biogeochem. Cycles 31 (6) (2017) 975–984, https://doi.org/10.1002/2016GB005583.
[3] E. Capuzzo, et al., A decline in primary production in the North Sea over 25 years, associated with reductions in zooplankton abundance and fish stock recruitment, Global Change Biol. 24 (1) (2018) e352–e364, https://doi.org/10.1111/gcb.13916.
[4] K.S. Johnson, M.B. Bif, Constraint on net primary productivity of the global ocean by Argo oxygen measurements, Nat. Geosci. (2021), https://doi.org/10.1038/s41561-021-00807-z.
[5] T.D. Eddy, et al., Energy flow through marine ecosystems: confronting transfer efficiency, Trends Ecol. Evol. 36 (1) (2021) 76–86, https://doi.org/10.1016/j.tree.2020.09.006.
[6] S.F. Henley, et al., Changing Biogeochemistry of the Southern Ocean and its Ecosystem Implications 7, 2020.
[7] I.M. Suthers, A.J. Richardson, D. Rissik, The importance of plankton, Plankt. A Guid. to Their Ecol. Monit. Water Qual. (2019) 1–13.
[8] C. Le Quéré, et al., Global carbon budget 2016, Earth Syst. Sci. Data 8 (2) (2016) 605–649, https://doi.org/10.5194/essd-8-605-2016.
[9] D.A. Smale, et al., Marine heatwaves threaten global biodiversity and the provision of ecosystem services, Nat. Clim. Change 9 (4) (2019) 306–312.
[10] P.K. Dunstan, et al., Global patterns of change and variation in sea surface temperature and chlorophyll a, Sci. Rep. 8 (1) (2018) 1–9.
[11] L. Kwiatkowski, et al., Twenty-first century ocean warming, acidification, deoxygenation, and upper-ocean nutrient and primary production decline from CMIP6 model projections, Biogeosciences 17 (13) (2020) 3439–3470.
[12] F. Boscolo-Galazzo, K.A. Crichton, S. Barker, P.N. Pearson, Temperature dependency of metabolic rates in the upper ocean: a positive feedback to global climate change? Global Planet. Change 170 (2018) 201–212.
[13] C. Fernández-González, G.A. Tarran, N. Schuback, E.M.S. Woodward, J. Arístegui, E. Marañón, Phytoplankton responses to changing temperature and nutrient availability are consistent across the tropical and subtropical Atlantic, Commun. Biol. 5 (1) (2022) 1–13.
[14] Q. Bao, et al., Role of carbon and nutrient exports from different land uses in the aquatic carbon sequestration and eutrophication process, Sci. Total Environ. 813 (2022), 151917.
[15] B.C. Franco, et al., Climate change impacts on the atmospheric circulation, ocean, and fisheries in the southwest South Atlantic Ocean: a review, Clim. Change 162 (4) (2020) 2359–2377.
[16] R.A. Watson, B.S. Green, S.R. Tracey, A. Farmery, T.J. Pitcher, Provenance of global seafood, Fish Fish. 17 (3) (2016) 585–595.
[17] A. Ferreira, P. Garrido-Amador, A.C. Brito, Disentangling environmental drivers of phytoplankton biomass off Western Iberia, Front. Mar. Sci. 6 (2019) 1–17, https://doi.org/10.3389/fmars.2019.00044.
[18] K. Nieto, F. Mélin, Variability of Chlorophyll-A Concentration in the Gulf of Guinea and its Relation to Physical Oceanographic Variables 151, The Authors, 2017, pp. 97–115.
[19] J. Abe, B.E. Brown, Towards a Guinea current large marine ecosystem commission, Environ. Dev. (2020), 100590.
[20] A. Newton, et al., Anthropogenic, direct pressures on coastal wetlands, Front. Ecol. Evol. 8 (2020) 144.
[21] M.J. Kennish, Management strategies to mitigate anthropogenic impacts in estuarine and coastal marine environments: a review, Open J. Ecol. 12 (10) (2022) 667–688.
[22] G. Kulk, et al., Primary production, an index of climate change in the ocean: satellite-based estimates over two decades, Rem. Sens. 12 (5) (2020) 1–26, https://doi.org/10.3390/rs12050826.
[23] A.S. Ayinde, E.O. Adeyemi, A.I. Fadipe, A.B. Hamzat, A. Ahmed, Influence of precipitation–runoff on oceanographic parameters in the gulf of Guinea, Int. J. Oceans Oceanogr. 14 (2) (2020) 183–196.
[24] S.M. Chiswell, J.R. Zeldis, M.G. Hadfield, M.H. Pinkerton, Wind-driven upwelling and surface chlorophyll blooms in Greater Cook Strait, N. Z. J. Mar. Freshw. Res. 51 (4) (2017) 465–489, https://doi.org/10.1080/00288330.2016.1260606.
[25] P. Xiu, F. Chai, E.N. Curchitser, F.S. Castruccio, Future changes in coastal upwelling ecosystems with global warming: the case of the California Current System, Sci. Rep. 8 (1) (2018) 1–9, https://doi.org/10.1038/s41598-018-21247-7.

[26] D.C. López-Sandoval, C.M. Duarte, S. Agustí, Nutrient and temperature constraints on primary production and net phytoplankton growth in a tropical ecosystem, Limnol. Oceanogr. 66 (7) (2021) 2923–2935.
[27] K. Richardson, J. Bendtsen, Vertical distribution of phytoplankton and primary production in relation to nutricline depth in the open ocean, Mar. Ecol. Prog. Ser. 620 (2019) 33–46.
[28] P. Flombaum, W.-L. Wang, F.W. Primeau, A.C. Martiny, Global picophytoplankton niche partitioning predicts overall positive response to ocean warming, Nat. Geosci. 13 (2) (2020) 116–120.
[29] D. Sharma, H. Biswas, S. Silori, D. Bandyopadhyay, Phytoplankton growth and community shift over a short-term high-CO2 simulation experiment from the southwestern shelf of India, Eastern Arabian Sea (summer monsoon), Environ. Monit. Assess. 194 (8) (2022) 1–16.
[30] D.A. Carozza, D. Bianchi, E.D. Galbraith, Metabolic impacts of climate change on marine ecosystems: implications for fish communities and fisheries, Global Ecol. Biogeogr. 28 (2) (2019) 158–169.
[31] R.F. Heneghan, et al., Disentangling diverse responses to climate change among global marine ecosystem models, Prog. Oceanogr. 198 (2021), 102659, https://doi.org/10.1016/j.pocean.2021.102659.
[32] H. Ducklow, et al., Marine pelagic ecosystem responses to climate variability and change, Bioscience 72 (9) (2022) 827–850.
[33] C.M. Petrik, C.A. Stock, K.H. Andersen, P.D. van Denderen, J.R. Watson, Large pelagic fish are most sensitive to climate change despite pelagification of ocean food webs, Front. Mar. Sci. 7 (2020), 588482.
[34] O. Karakuş, C. Völker, M. Iversen, W. Hagen, J. Hauck, The role of zooplankton grazing and nutrient recycling for global ocean biogeochemistry and phytoplankton phenology, J. Geophys. Res. Biogeosciences 127 (10) (2022), e2022JG006798.
[35] K.M. Krumhardt, et al., Potential predictability of net primary production in the ocean, Global Biogeochem. Cycles 34 (6) (2020), e2020GB006531, https://doi.org/10.1029/2020GB006531.
[36] D.P. Tittensor, et al., A protocol for the intercomparison of marine fishery and ecosystem models: fish-MIP v1. 0, Geosci. Model Dev. (GMD) 11 (4) (2018) 1421–1442.
[37] K.S. Davies-Vollum, D. Raha, D. Koomson, Climate Change Impact and Adaptation: Lagoonal Fishing Communities in West Africa BT - African Handbook of Climate Change Adaptation, in: N. Oguge, D. Ayal, L. Adeleke, I. da Silva (Eds.), Springer International Publishing, Cham, 2021, pp. 2221–2245.
[38] A.M. Dahunsi, F.F. Bonou, O.A. Dada, E. Baloïtcha, Spatio-temporal trend of past and future extreme wave climates in the gulf of Guinea driven by climate change, J. Mar. Sci. Eng. 10 (11) (2022) 1581.
[39] E.S. Nyadjro, B.A.K. Foli, K.A. Agyekum, G. Wiafe, S. Tsei, Seasonal variability of Sea Surface salinity in the NW gulf of Guinea from SMAP satellite, Remote Sens. Earth Syst. Sci. 5 (1) (2022) 83–94.
[40] Z. Sohou, et al., Seasonal and inter-annual ONSET Sea Surface temperature variability along the northern coast of the gulf of Guinea, Reg. Stud. Mar. Sci. 35 (2020), 101129.
[41] A. Sylla, J. Mignot, X. Capet, A.T. Gaye, Weakening of the Senegalo–Mauritanian upwelling system under climate change, Clim. Dynam. 53 (7) (2019) 4447–4473.
[42] S.L. Chune, L. Aouf, L. Bruno, A. Dalphinet, Global High Resolution Production Centre GLOBAL_REANALYSIS_WAV_001_032, 2019.
[43] J. Lamouroux, C. Perruche, A. Mignot, J. Paul, C. Szczypta, Quality Information Document, 2019.
[44] C. Perruche, C. Szczypta, J. Paul, M. Drévillon, Global Production Centre GLOBAL_REANALYSIS_BIO_001_029, 2019.
[45] H.L. Varona, F. Hernandez, A. Bertrand, M. Araujo, Monthly anomaly database of atmospheric and oceanic parameters in the tropical Atlantic ocean, Data Brief 41 (2022), 107969.
[46] C.A. Greene, et al., The climate data toolbox for MATLAB, G-cubed 20 (7) (2019) 3774–3781.
[47] N.A. Sweijd, A.J. Smit, Trends in sea surface temperature and chlorophyll-a in the seven African Large Marine Ecosystems, Environ. Dev. 36 (2020), 100585.
[48] S.M. Chiswell, P.J.H. Sutton, Relationships between long-term ocean warming, marine heat waves and primary production in the New Zealand region, N. Z. J. Mar. Freshw. Res. 54 (4) (2020) 614–635.
[49] G. Li, L. Cheng, J. Zhu, K.E. Trenberth, M.E. Mann, J.P. Abraham, Increasing ocean stratification over the past half-century, Nat. Clim. Change 10 (12) (2020) 1116–1123.
[50] A. Supply, J. Boutin, G. Reverdin, J.L. Vergely, H. Bellenger, Variability of satellite sea surface salinity under rainfall, Adv. Glob. Chang. Res. 69 (2020) 1155–1176, https://doi.org/10.1007/978-3-030-35798-6_34.
[51] R. Curry, B. Dickson, I. Yashayaev, A change in the freshwater balance of the Atlantic Ocean over the past four decades, Nature 426 (6968) (2003) 826–829, https://doi.org/10.1038/nature02206.
[52] O.J. Houndegnonto, N. Kolodziejczyk, C. Maes, B. Bourlès, C.Y. Da-Allada, N. Reul, Seasonal variability of freshwater plumes in the eastern gulf of Guinea as inferred from satellite measurements, J. Geophys. Res. Ocean. 126 (5) (2021) 1–27, https://doi.org/10.1029/2020JC017041.
[53] C.Y. Da-Allada, G. Alory, Y. du Penhoat, J. Jouanno, M.N. Hounkonnou, E. Kestenare, Causes for the recent increase in sea surface salinity in the north-eastern Gulf of Guinea, Afr. J. Mar. Sci. 36 (2) (2014) 197–205, https://doi.org/10.2989/1814232X.2014.927398.
[54] P.J. Durack, S.E. Wijffels, Fifty-Year trends in global ocean salinities and their relationship to broad-scale warming, J. Clim. 23 (16) (2010) 4342–4362, https://doi.org/10.1175/2010JCLI3377.1.
[55] A.N. Dossa, G. Alory, A.C. da Silva, A.M. Dahunsi, A. Bertrand, Global analysis of coastal gradients of sea surface salinity, Rem. Sens. 13 (13) (2021), https://doi.org/10.3390/rs13132507.
[56] M.S. Martins, D. Stammer, Interannual variability of the Congo river plume-induced Sea Surface salinity, Rem. Sens. 14 (4) (2022) 1013, https://doi.org/10.3390/rs14041013.
[57] W.W. Gregg, C.S. Rousseaux, Global ocean primary production trends in the modern ocean color satellite record (1998–2015), Environ. Res. Lett. 14 (12) (2019), 124011.
[58] G. Wiafe, E.S. Nyadjro, Satellite observations of upwelling in the Gulf of Guinea, Geosci. Rem. Sens. Lett. IEEE 12 (5) (2015) 1066–1070.
[59] EPA, Report on the Environment, 2019. http://www.epa.gov/roe/.
[60] H. Auricht, L. Mosley, M. Lewis, K. Clarke, Mapping the long-term influence of river discharge on coastal ocean chlorophyll-a, Remote Sens. Ecol. Conserv. 8 (5) (2022) 629–643, https://doi.org/10.1002/rse2.266.
[61] O.A. Nubi, E.A. Ajao, E.O. Oyewo, J.P. Unyimadu, Nutrient levels in Guinea current large marine ecosystem (GC-LME) waters, Sci. World J. 3 (2) (2008).
[62] S.F. Dan, S.-M. Liu, E.C. Udoh, S. Ding, Nutrient biogeochemistry in the cross river estuary system and adjacent gulf of Guinea, south east Nigeria (west africa), Continent. Shelf Res. 179 (2019) 1–17.
[63] A. Bichet, A. Diedhiou, Less frequent and more intense rainfall along the coast of the Gulf of Guinea in West and Central Africa (1981 2014), Clim. Res. 76 (3) (2018) 191–201.
[64] M.O. Kadiri, J.U. Ogbebor, O.A. Omoruyi, T. Unusiotame-Owolagba, Chlorophyll a measurement as an index of phytoplankton bloom and primary production in the Gulf of Guinea, Nigeria, West Africa, Stud. Univ. Babes-Bolyai. Biol. 64 (2) (2019) 97–109, https://doi.org/10.24193/subbbiol.2019.2.08.